Direct Numerical Simulation of High Speed Jet Atomization

S.Zaleski and T. Boeck

LMM, UPMC,
4 place Jussieu, 75005 Paris, France
zaleski@lmm.jussieu.fr

Abstract : The LMM interface team performed various investigations in the field of theoretical and numerical analysis of atomization. The main tool was the SURFER code. Special emphasis was put on application to cryogenic rocket engines. The goal of this work is a better understanding of the fundamental mechanisms leading to droplet production in the near nozzle region of the injector. The principal physical hypothesis is that the droplet production originates in a Kelvin Helmholtz instability in the approximately parallel and strongly sheared flow of gas and liquid oxygen near the injector exit.

1 Introduction

Broad agreement exists in the scientific community on the origin of the atomization phenomenon in rocket engines. This would be due to the aerodynamic effect on the sheared liquid-gas interface, provoking a Kelvin-Helmholtz type instability [4, 9]. The simplest version of this theory assumes a staircase-like velocity profile and the temporal development of the instability. It predicts a critical Weber number above which instability develops [1].

A more realistic theory is obtained assuming a piecewise linear velocity profile. The thickness of boundary layers near the interface may then be related to the thickness of the boundary layers created by the upstream near-wall flow which creates the profile near the nozzle exit. Boundary layers then develop under the action of viscosity [13]. These profiles were employed in the theoretical work of E. Villermaux and coworkers and lead to good agreement with experiments. On the other hand precise quantitative agreement was difficult to find between linear theory and numerical simulations.

Recently a much more realistic linear theory of atomization was developed by Phil Yecko and the authors [14, 15, 7]. It uses error function profiles and solves the full linearized viscous equations, i.e. the Orr-Sommerfeld equations. The error function profiles have advantages in the comparison with numerical simulation as they are slowly variable at small viscosity. Excellent agreement is then obtained with the full numerical simulation [7].

An interesting feature of the Orr-Sommerfeld theory is that one obtains, for sufficiently large Reynolds numbers, two new instability modes, one for the gas and one for the liquid [14, 15].

Modern numerical methods allow to go beyond linear stability theory and simulate the full non-linear development of the instability. The VOF method discussed in this

paper are particularly well adapted to the study of atomization. We had already applied it to secondary atomization, i.e. atomization of droplets caught in a strong relative gas velocity in ref [16]. Outside activities in our group, one may cite those of the Tryggvason group who uses markers methods to simulate the nonlinear stage of the Kelvin-Helmholtz instability [12].

2 Numerical methods

The interface team at LMM has developed a set of numerical methods put together in the SURFER codes. These methods are mostly adapted to the tracking of interfaces and the solution of the Navier Stokes equations with two fluid phases [5, 10, 2]. The framework is direct numerical simulation rather than the use of turbulence models such $k-\epsilon$ models. It is a realistic choice in line with the improvement in computational methods and computer equipment. We used the Volume of Fluid (VOF) method, where the presence of liquid in a cell is characterized by a volume fraction. In return for moderate complexity, the VOF method can be used in three space dimensions with good accuracy.

Interfaces are reconstructed by planes cutting the cubic cells of the grid. The planar reconstruction is characteristic of the VOF-Piecewise Linear Interface calculation or VOF-PLIC. The volume fraction is then propagated by a fractional step method. Various tests have demonstrated the accuracy of this geometrical approach for simple objects subject to translation or rotation. [11]. Upon topology changes, for instance during droplet coalescence or breakup in a multiphase flow, various short range molecular effects may become relevant: van der Waals forces, effects of surfactant molecules etc... The VOF methods effects reconnections in a simplified way that mimics the microscopic physics. This is an important advantages compared to other methods such as connected markers that are forced to stop when interfaces tend to reconnect or are excessively deformed.

3 Linear stability theory and results

In what follows we first investigate the full temporal stability of the co-flowing jets, with a particular view toward cryogenic fluids.

3.1 Kelvin-Helmholtz Instability

The Kelvin-Helmholtz instability of two rapidly moving fluids with different velocities can be viewed on different levels of abstraction, some of which are shown schematically in Fig. 1. Neglecting viscosity, one can consider the situation of Fig. 1a, namely a simple step velocity profile as the generic basic flow. This is not possible for real fluids, where the velocity must be continuous across the interface. This leads naturally to the broken-line basic velocity profile of Fig. 1b, where the boundary layers next to the interface ensure continuity of the horizontal velocity. While more realistic than the step profile, one still cannot take the effects of viscosity properly into account with this profile because it does not represent a solution of the viscous Navier-Stokes equations.

For a viscous stability analysis it therefore becomes necessary to consider a basic velocity profile shown in Fig. 1c, which is composed of two error function profiles, namely

$$U_l = U_l^\star \mathrm{erf}(y/\delta_l), \qquad U_g = U_g^\star \mathrm{erf}(y/\delta_g). \tag{1}$$

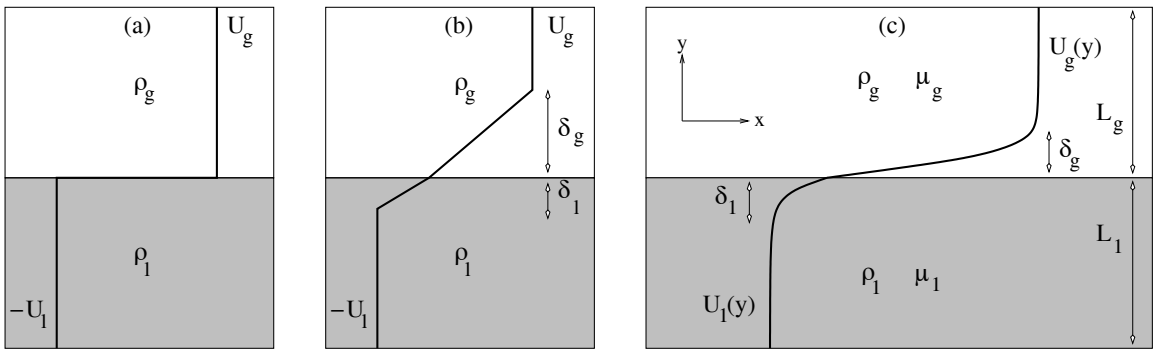

Figure 1: *Basic velocity profiles: (a) step profile, (b) piecewise linear profile, (c) error function profile. The interface position is at $y = 0$. For (b) and (c), the horizontal velocity at the interface is assumed zero, which is permitted because of Galilean invariance with respect to the streamwise coordinate.*

This profile has been already considered in earlier work by one of the authors ref. [15]. The error function profiles can be considered as approximate solutions of the boundary layer equations [8]. Assuming that the Kelvin-Helmholtz instability proceeds much faster than the downstream evolution of the basic profile, one can consider the profile as frozen and perform a viscous temporal stability analysis in the same way as for the time-independent inviscid profiles in Fig. 1a,b. We note that the asymptotic velocities $U_g^\star$ and $U_l^\star$ in the viscous problem are coupled to the boundary layer thicknesses δ_g and δ_l because of the shear stress continuity on the interface, i.e.

$$\frac{\mu_l U_l^\star}{\delta_l} = \frac{\mu_g U_g^\star}{\delta_g}. \tag{2}$$

The same condition can be imposed in the piecewise linear profile although the inviscid problem does not require it.

We consider the linear stability problem in two dimensions, i.e. perturbations about the basic flow of the form

$$\psi_l(x,y,t) = \exp(i\alpha(x-ct))\phi_l(y), \quad \psi_g(x,y,t) = \exp(i\alpha(x-ct))\phi_g(y), \tag{3}$$

where ψ_l and ψ_g are the stream functions of the velocity perturbations in the respective fluid, α denotes the wave number and c the complex phase velocity. Linearization about the basic velocity profile provides the appropriate equations and boundary conditions for the functions $\phi_l(y)$ and $\phi_g(y)$, which can be found in various references such as [15]. In the inviscid case, one has to ensure continuity of the perturbations in the vertical velocity and the normal stress at the interface. In addition, continuity of the shear stress and horizontal velocity perturbations must be satisfied in the viscous case.

Apart from the interface, one also must impose boundary conditions on the outer boundaries, ideally at $y = \pm\infty$. This is easy for the inviscid piecewise linear problem, which can be solved analytically, and where one demands that the velocity perturbations decay for $y \to \pm\infty$.

The viscous (and inviscid) stability problems for the error function profiles can only be solved numerically, and one has to impose conditions at some finite vertical distance from the interface. One can take the full domain into account by an approach which we explain

briefly for the gas layer. We divide it into the intervals $0 < y < L_g$ and $L_g < y < \infty$. In the latter interval we assume a constant basic flow and solve the stability problem analytically. The boundary conditions on $y = L_g$ for the numerical solution in the finite interval $0 < y < L_g$ are the appropriate matching conditions to the outer analytical solution, namely continuity of horizontal velocity and normal stress perturbations for the inviscid case, and, in addition, continuity of shear and horizontal velocity perturbations for the viscous case. The same technique is used in the inviscid case for the liquid layer, where we apply the matching conditions to the analytical solution on $y = -L_l$. For the viscous case we assume a fixed wall at $y = -L_l$ for simplicity. This is justified because the gas layer is more important dynamically for the physical parameters typical of airblast atomization.

The linear eigenvalue problem for the phase velocity c with given physical parameters and wave number α in the domain $-L_l < y < L_g$ is solved numerically using a Chebyshev collocation method. The eigenfunctions ϕ_l and ϕ_g are expanded in Chebyshev polynomials. The algebraic eigenvalue problem is obtained by substitution of the expansions into the equations for ϕ_l and ϕ_g and evaluation at collocation points chosen to ensure spectral accuracy. For the solution of the resulting general algebraic eigenvalue problem we use the NAG library function F02GJF.

3.2 Results

We shall use dimensionless units for the representation of the results which are mostly based on the gas layer parameters. Lengths will be measured in units of δ_g and velocities in units of $U_g^\star$, whereby the scale of time is defined as well. As set of dimensionless parameters we use the ratios of the material properties and lengthscales

$$m = \frac{\mu_g}{\mu_l}, \quad n = \frac{\delta_g}{\delta_l}, \quad r = \frac{\rho_g}{\rho_l} \tag{4}$$

of both layers, and the gas Reynolds and Weber numbers

$$Re = \frac{\rho_g U_g^\star \delta_g}{\mu_g}, \quad We = \frac{\rho_g \left(U_g^\star\right)^2 \delta_g}{\sigma}. \tag{5}$$

Gravity is not taken into account, i.e. the results will apply for infinite Froude number.

In the following we consider two sets of values for m and r which approximately correspond to the combinations air/water and hydrogen/liquid oxygen, namely ($r = 0.001, m = 0.02$) and ($r = 0.02, m = 0.025$). These are relevant for laboratory experiments on airblast atomization and for cryogenic fuels in rocket motors. With these parameters fixed one still has the parameters n, Re and We to consider. The Reynolds number is inconsequential for the inviscid case, for which we present several stability curves. It is well known that for inviscid stability theory the growth rates αc_i depend only weakly on the precise form of the profile. This is illustrated in Fig. 2, which compares results for the continuous error function profile with the broken line profile for equal thicknesses of the liquid and gas boundary layers. The Weber numbers are typical of configurations discussed in ref. [3] with U_g of the order of 100 m/s and δ_g of the order of 0.1 mm for air/water and 1 μm for the cryogenic fuels. Larger values of n were also tried and similar agreement was observed.

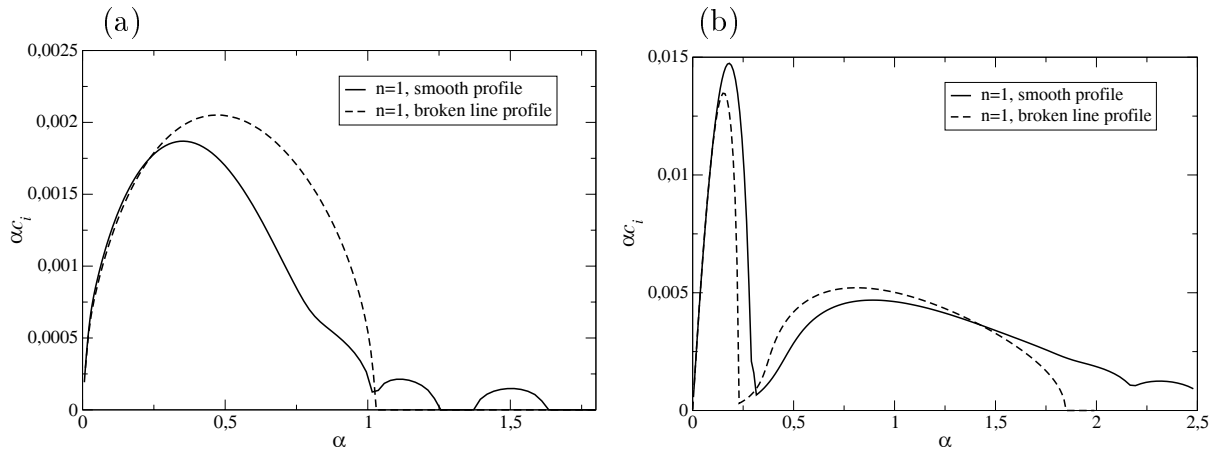

Figure 2: *Comparison of inviscid stability results for the error functions profile and broken line profile for the air/water case and* $We = 10$ *(a) and the cryogenic fuel case with* $We = 200$ *(b).*

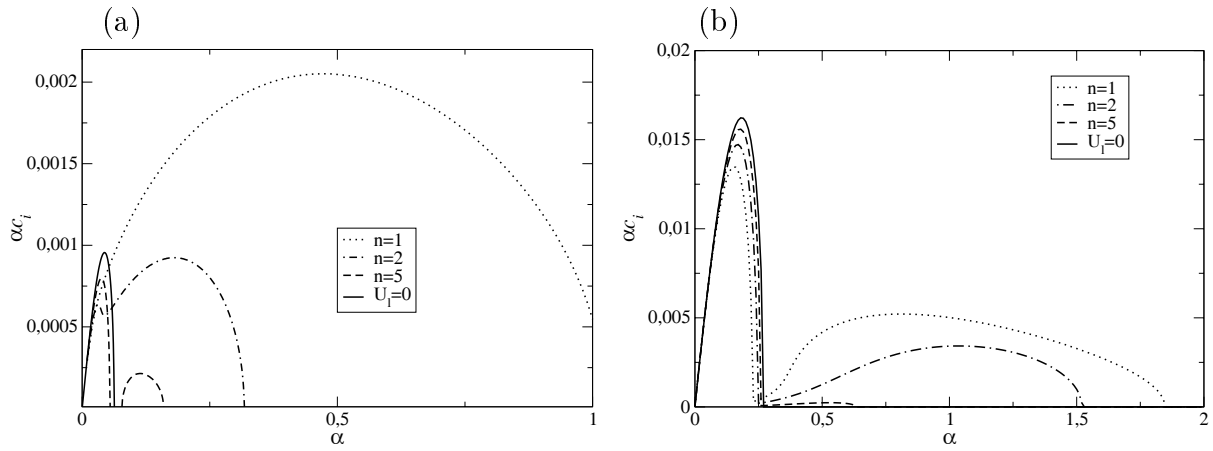

Figure 3: *Effect of varying* n *on inviscid stability results for the broken line profile air/water case and* $We = 10$ *(a) and the cryogenic fuel case with* $We = 200$ *(b).*

Because the detailed shape of the velocity profile does not matter much, we shall simply use the broken line profile to study the effect of varying n in the inviscid situation. Figure 3 shows the curves for $U_l = 0$ as continous lines, which correspond to the case when the liquid has no boundary layer. For the air/water case we observe emergence of another branch at higher α when n is decreased, which is already dominant for $n = 2$ for the air/water parameters. This is much less pronounced for the cryogenic case, where the limit $U_l = 0$ still gives a good prediction for the most unstable wavelength and growthrate, but the same trend is present.

Viscous stability calculations for the smooth error functions profile show a reversal of this trend for the air/water system as shown in Fig. 4(a). In addition, one finds a large quantitative difference between the inviscid and viscous growth rates. Depending on n, the most unstable wavelength and the associated growth rate are larger by a factor of nearly 10 when compared with the inviscid result without gas boundary layer. The factors are smaller for the cryogenic case, and no significant dependence on n is observed in for $1 \leq n \leq 5$. The Reynolds numbers are again chosen to be typical of experimental

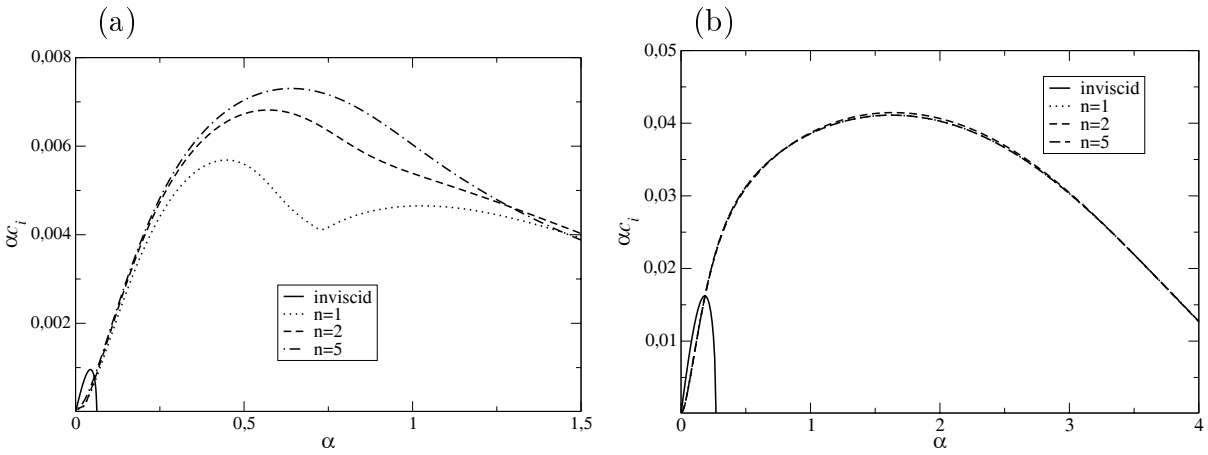

Figure 4: *Effect of varying n on viscous stability results for the error functions profile for the air/water case with $Re = 500$, $We = 10$ (a) and the cryogenic fuel case with $Re = 1000$, $We = 200$ (b). Note that $L_g = L_l = 5$ in the computation.*

configurations discussed in ref. [3].

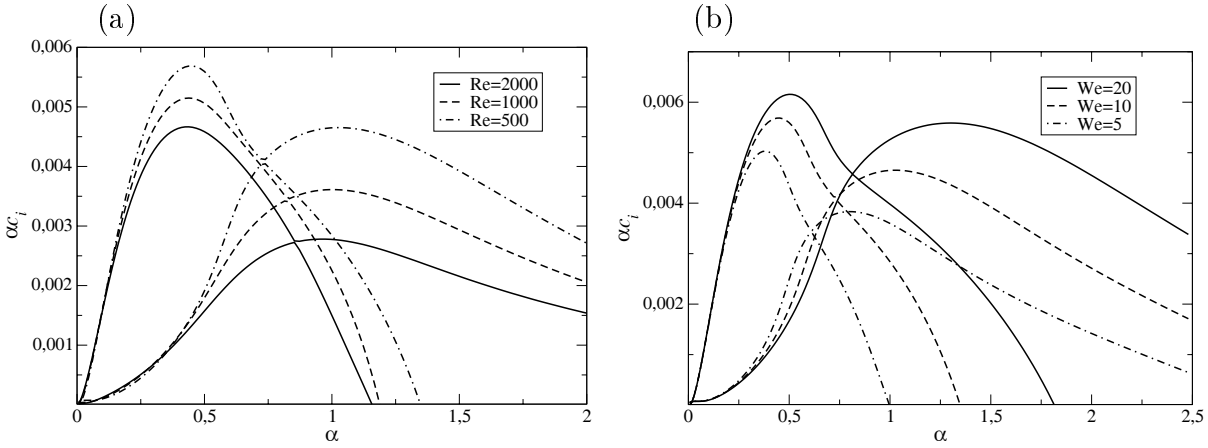

Figure 5: *Effect of varying Re and We on viscous stability results for the air/water system with error functions profile and $n = 1$. (a) $We = 10$ fixed, (b) $Re = 500$ fixed.*

Let us now consider the dependence on the Reynolds and Weber number for the two sets of parameters for fixed $n = 1$. For the air/water system shown in Fig. 5 we see that increasing the Reynolds number for fixed $We = 10$ reduces the maximum growthrate but has not much effect on the most unstable wavelength. Not surprisingly, we see that increasing the Weber number leads to larger maximum growthrate and wavelength at fixed $Re = 500$.

The cryogenic case of Fig. 6 is different because there is only one unstable branch present, but the general trends are the same as for the air/water system.

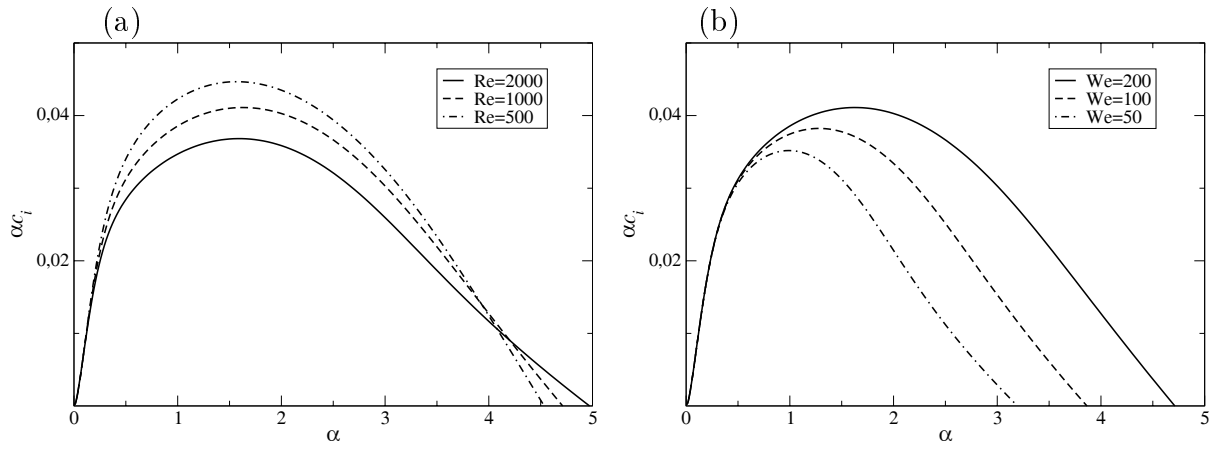

Figure 6: *Effect of varying Re and We on viscous stability results for the cryogenic case with error functions profile and $n = 1$. (a) $We = 200$ fixed, (b) $Re = 1000$ fixed.*

4 Fully nonlinear calculations:spatial development of the instability

At present we have not yet been able to match the linear theory above with full direct numerical simulation of the instability. However good agreement with linear theory exists in two dimensional simulations of spatially periodic patterns, which have been reported elsewhere [7]

We also performed simulations showing the spatial development of the instability. These simulations should allow comparisons with experimental observations in various locations near the nozzles, such as measurements of probability density functions (pdf's) of droplet sizes.

Our main observation is a very important effect of the turbulence level at the origin of the jet. We modeled turbulence in the nozzle inlet as prescribed vortices which are forced in addition to the entering fluid average velocity. More details on these calculations may bve found in ref. [6].

5 Conclusion and perspectives

We have shown that the instabilities leading to atomization exhibit both a complex structure of linear modes and a rich nonlinear development into filaments and droplets. Future work should concentrate on matching the predicted wavelength in linear theory and the observed nonlinear development.

Three dimensional spatial simulations are now possible, but not yet very accurate, due to the large number of grid points needed to represent the smallest droplets. The interested reader may browse the web page http://www.lmm.jussieu.fr/∼zaleski/gouttes.html. An increase in about a factor of 100 in computer power is necessary to reach a comparable grid size in 3D as is currently available in 2D. Given the current pace of improvement in CPUs and the possibility of using parallel computations, this capability should be available in less than ten years.

Other improvements could be useful and especially the ability to simulate complex

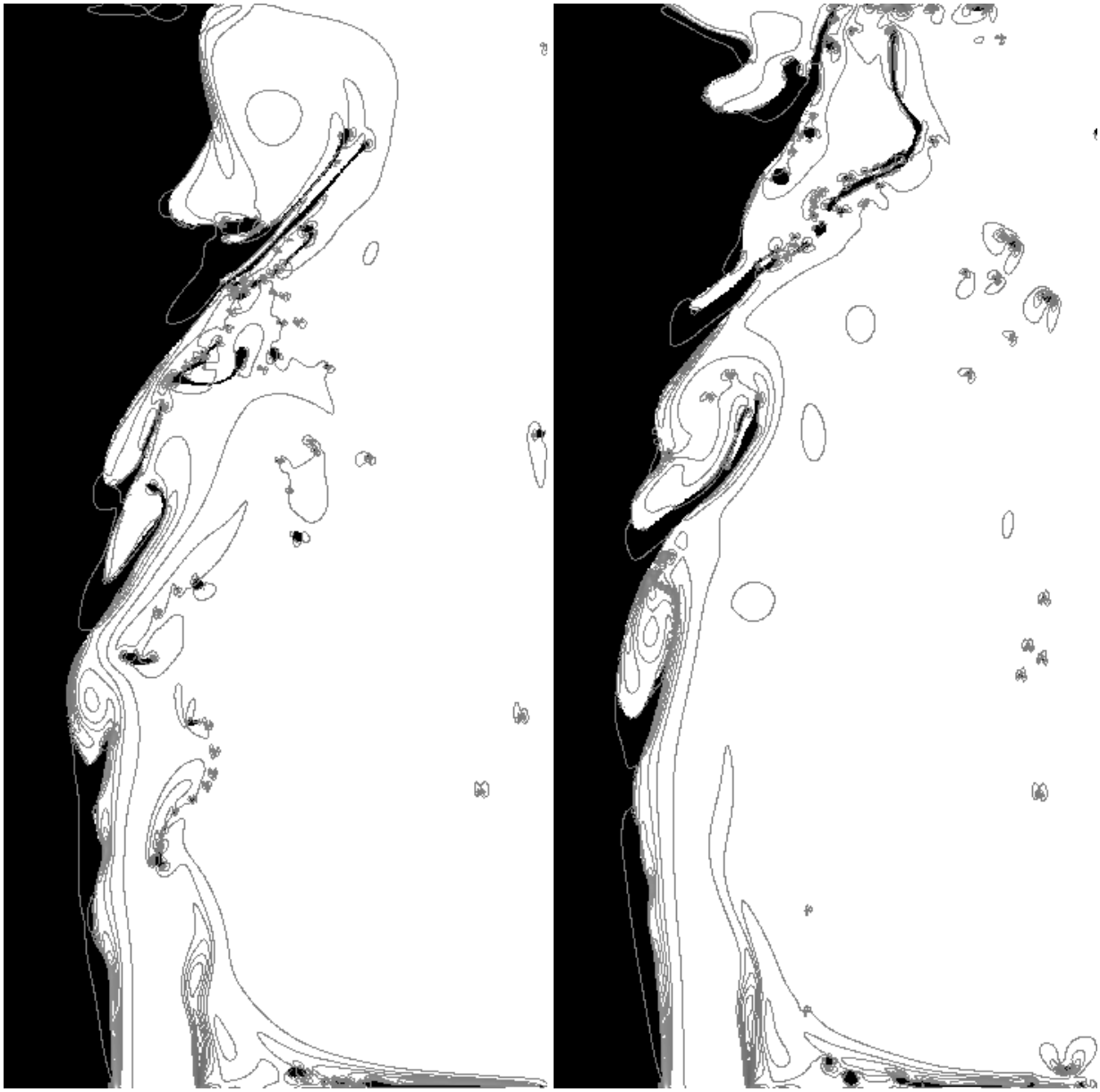

Figure 7: *A simulation of the spatial development of the instability. The conditions are* $\mathrm{Re}_G = 1160$ *(based on the diameter of the gas jet)* $\mathrm{Re}_L = 60$ *(based on the diameter of the liquid jet),* $\mathrm{We}_G = 387$ *(based on the diameter of the gas) and* $rho_L/rho_G = 10$.

solid boundaries such as the ones that exist upstream inside nozzles. New codes are being developed with the capability of treating complex boundaries, parallelization and adaptive grid refinement, such as the GFS or Gerris code, available at http://gfs.sf.net.

References

1. S. Chandrasekhar. *Hydrodynamic and hydromagnetic stability.* Oxford Univ. Press, Oxford, 1961.

2. D. Gueyffier, A. Nadim, J. Li, R. Scardovelli, and S. Zaleski. Volume of fluid interface tracking with smoothed surface stress methods for three-dimensional flows. *J. Comput. Phys.*, 152:423–456, 1999.

3. Emil J. Hopfinger. Atomisation d'un jet liquide par un jet de gaz coaxial: Un bilan des connaissances acquises. In *Combustion dans les moteurs fusées, Toulouse, 26-28 June 2001*, pages 34–47. CEPADUES Editions, Toulouse, 2001.

4. J. W. Hoyt and J.J. Taylor. Waves on water jets. *J. Fluid Mech.*, 83:119–127, 1977.

5. B. Lafaurie, C. Nardone, R. Scardovelli, S. Zaleski, and G. Zanetti. Modelling merging and fragmentation in multiphase flows with SURFER. *J. Comput. Phys.*, 113:134–147, 1994.

6. A. Leboissetier and S. Zaleski. Influence des conditions amont turbulentes sur l'atomisation primaire. *Combustion (Revue des Sciences et Techniques de Combustion)*, 2:75–87, 2002.

7. Jie Li, Enrique López-Pagés, Philip Yecko, and Stéphane Zaleski. Droplet formation in sheared liquid-gas layers. submitted to Theor. Comput. Fluid Mech., 2003.

8. R. C. Loch. *Quart. J. Mech. Appl. Math.*, 4:42–63, 1951.

9. D.R. Reitz and F. Bracco. Mechanism of atomisation of a liquid jet. *Physics of Fluids*, 25:1730–1742, 1982.

10. R. Scardovelli and S. Zaleski. Direct numerical simulation of free-surface and interfacial flow. *Annu. Rev. Fluid Mech.*, 31:567–603, 1999.

11. R. Scardovelli and S. Zaleski. Interface reconstruction with least-square fit and split lagrangian-eulerian advection. *Int J. Numer. Meth. Fluids*, 41:251–274, 2002.

12. W. Tauber, S. O. Univerdi, and G. Tryggvason. The non-linear behavior of a sheared immiscible fluid interface. *Phys. Fluids*, 14:2871, 2002.

13. E. Villermaux. On the role of viscosity in shear instabilities. *Physics of Fluids*, 10(2):368–73, 1998.

14. P. Yecko and S. Zaleski. Two-phase shear instability: waves, fingers and drops. *Annals of the New York Academy of Sciences*, 898:127–143, 1999.

15. P. Yecko, S. Zaleski, and J.-M. Fullana. Viscous modes in two-phase mixing layers. *Phys.Fluids*, 14:4115–4122, 2002.

16. S. Zaleski, Jie Li, and S. Succi. Two-dimensional Navier-Stokes simulation of deformation and breakup of liquid patches. *Phys. Rev. Lett.*, 75:244–247, 1995.